

Article

Seasonal Hypoxia Enhances Benthic Nitrogen Fixation and Shapes Specific Diazotrophic Community in the Eutrophic Marine Ranch

Cheng Yao ^{1,2}, Qianqian Zhang ¹, Xianbiao Lin ³, Jianmin Zhao ^{1,*} and Xiaoli Zhang ^{1,*} ¹ Yantai Institute of Coastal Zone Research, Chinese Academy of Sciences, Yantai 264003, China² University of Chinese Academy of Sciences, Beijing 100049, China³ Frontiers Science Center for Deep Ocean Multispheres and Earth System, Key Laboratory of Marine Chemistry Theory and Technology, Ministry of Education, Ocean University of China, Qingdao 266100, China

* Correspondence: jmzhao@yic.ac.cn (J.Z.); xlzhang@yic.ac.cn (X.Z.)

Abstract: Recently, a growing number of studies have confirmed that biological nitrogen fixation is also an important reactive nitrogen source in coastal regions. However, how benthic nitrogen fixation and diazotrophic community in coastal regions respond to seasonal hypoxia remains largely unknown. In this study, we investigated the spatiotemporal pattern of potential nitrogen fixation rate and diazotrophic abundance and community in sediments of a eutrophic marine ranch experiencing summer hypoxia using ¹⁵N tracing and high throughput sequencing techniques. The results showed that potential nitrogen fixation rates ranged from 0.013 to 10.199 $\mu\text{mol kg}^{-1} \text{h}^{-1}$, and were significantly enhanced by summer hypoxia (ANOVA, $p < 0.05$). However, *nifH* gene abundance peaked in June. The diazotrophic community was dominated by Geobacteraceae (>60%), followed by Desulfobulbaceae (13.61%). Bottom water oxygen, pH, Chl-*a* concentration, and sediment NH_4^+ significantly regulated benthic nitrogen fixation, while the variation of diazotrophic community was explained by sediment TOC, TN, and Fe content ($p < 0.05$). This study highlighted that hypoxia stimulated benthic nitrogen fixation, which counteracted the nitrogen removal by denitrification and anammox, and could further aggregate eutrophication of the coastal marine ranch. Moreover, the result emphasized the importance of nitrogen fixation in coastal regions for the global N budget.

Keywords: benthic nitrogen fixation; coastal marine ranch; seasonal hypoxia; diazotrophs; iron-reducing



Citation: Yao, C.; Zhang, Q.; Lin, X.; Zhao, J.; Zhang, X. Seasonal Hypoxia Enhances Benthic Nitrogen Fixation and Shapes Specific Diazotrophic Community in the Eutrophic Marine Ranch. *Processes* **2023**, *11*, 138. <https://doi.org/10.3390/pr11010138>

Academic Editor: Zhi-Yong Li

Received: 17 November 2022

Revised: 23 December 2022

Accepted: 30 December 2022

Published: 3 January 2023



Copyright: © 2023 by the authors. Licensee MDPI, Basel, Switzerland. This article is an open access article distributed under the terms and conditions of the Creative Commons Attribution (CC BY) license (<https://creativecommons.org/licenses/by/4.0/>).

1. Introduction

N_2 fixation converts N_2 to bioavailable ammonium, an essential source of new nitrogen into the marine [1]. It has been estimated that N_2 fixation contributes about 163 Tg N yr^{-1} to the global marine N budget [2]. Marine N_2 fixation has received increasing attention in recent decades because of its significant contribution to regulating the primary productivity and nitrogen balance of marine environments [1]. Traditionally, the oligotrophic open oceans have been considered as hotspots for N_2 fixation [3,4], where large filamentous and heterocystous cyanobacteria are principal diazotrophs. However, recent evidence suggests that biological N_2 fixation is also a significant process within coastal waters and even sediments [5–7], where unicellular cyanobacteria and heterotrophic bacteria contributed significantly to N_2 fixation. Therefore, an enhanced understanding of N_2 fixation rates and diazotroph diversity patterns within coastal ecosystems is required to inform models of marine N availability on global scales.

In coastal ecosystems, high organic matter loading promotes high rates of microbial activity and high oxygen consumption, and when combined with restricted water circulation, hypoxia (dissolved oxygen < 62.5 μM) can develop [8]. It is estimated that the hypoxic area in world-wide coastal regions is over 24,500 km^2 [9]. Moreover, these hypoxic

regions are expanding due to global warming and anthropogenic eutrophication [9]. Under hypoxic conditions, the N loss process denitrification was generally enhanced [10,11], and in some situations, anammox can also play an important role [12,13], but how the N₂ fixation process responds to hypoxia occurrence remains unclear. Fernandez et al. (2011) observed that N₂ fixation rates in the subsurface oxygen-deficient waters were five times higher than those in the oxic euphotic waters in the eastern tropical South Pacific (ETSP) oxygen-minimum zone [14]. Gier et al. (2016) reported that N₂ fixation rates in OMZ sediments were similar to rates measured in other organic-rich sediments [15]. However, the highest sediment N₂ fixation rates were detected when hypoxia developed in deep water in the Eckernförde Bay [16]. These conflicting results suggest that more extensive studies about N₂ fixation in hypoxic regions are needed to better understand the influence of hypoxia on marine nitrogen balance. In particular, in the coastal region where nitrogen input contributed significantly to the development of hypoxia, understanding the feedback of the N₂ fixation process on hypoxia will expand our knowledge on the ecological consequences of hypoxia and give advice to managers on maintaining sustainable development of coastal ecosystems.

The widespread application of molecular surveys targeting the *nifH* gene (encoding a subunit of the nitrogenase enzyme complex) indicated high diversity of marine diazotrophs [14,15,17]. Vahtera et al. (2007) suggested that enhanced internal loading of phosphorus and the removal of dissolved inorganic nitrogen by hypoxia promoted nitrogen-fixing cyanobacteria blooms in the Baltic Sea [18]. In the deep hypoxic waters of the Southern California Bight, Alpha- and Gamma-proteobacteria and putative sulfate-reducing bacteria were reported to be primary diazotrophs [19]. Bertics et al. (2013) found that some sediment sulfate reducing bacteria conducted nitrogen fixation in the hypoxic Eckernförde Bay [16]. Nonetheless, how benthic diazotroph community shifts in response to the development of seasonal hypoxia in coastal ecosystems is poorly understood.

The northern coast of the Yellow Sea is one of the main mariculture areas in northern China. Excessive organic matter and nitrogen inputs from farming activities have led to bottom water hypoxia during summer with high temperature and rain since 2013. This series of hypoxic events caused significant changes in benthic organisms [20], planktons [21], and bacterial communities [22], but information on seasonal changes in benthic nitrogen fixation activity and diazotroph community are limited. In this study, surface sediment samples were collected from the ranching area from June to November 2017, and environmental parameters, potential nitrogen fixation (NF) rates, as well as *nifH* gene abundance and compositions were characterized. We aimed to describe the dynamics of benthic nitrogen fixation responding to the development of seasonal hypoxia, and to explore the possible driving mechanism of benthic nitrogen fixation in coastal ecosystems. The results will facilitate a better understanding of the N-cycling process in coastal systems during hypoxia events and provide a reference for ecological assessments of the impact of hypoxia on the coastal ecological functions.

2. Materials and Methods

2.1. Sample Collection

The study area is located in Muping, Yantai, the offshore of North Yellow Sea (37°31'12" N; 121°48'36" E) (Figure 1). The Muping Marine Ranch has a cultivation area of about 12.16 km² and a water depth of 12–16 m. The area is affected by the East Asian monsoon climate with strong variations in seawater temperature, salinity, and water column stratification during the year [20]. Seasonal hypoxia has occurred in this area every summer since 2013, which occurred generally from July, persisting until the end of August, and gradually evaporated after September. Sampling was performed at seven sites (16, 17, 18, 19, 20, S8, and S9) along a section extending from the coast to offshore through the ranch during five cruises (June, July, August, September, and November) in 2017 (Figure 1). Surface sediments (0–5 cm) were collected with a gravity box corer (Uwitech, Austria), and triple subsamples were taken from each site and mixed immediately. Part of the sediments

were stored in liquid nitrogen for subsequent molecular analysis and environmental factor determination, and the remaining part was stored at 4 °C for incubation experiments within 24 h.

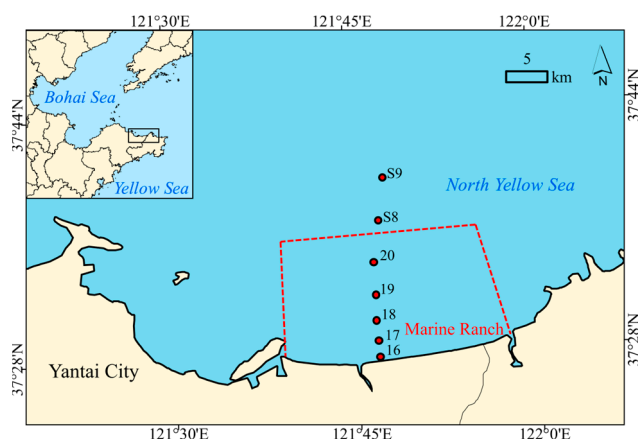


Figure 1. Study area and sampling sites.

2.2. Environmental Parameters Analysis

The environmental parameters, including depth, temperature, salinity, dissolved oxygen (DO), pH and chlorophyll-*a* (Chl-*a*) of bottom waters, grain size, the total organic carbon (TOC) and nitrogen (TN), the exchangeable NH_4^+ , NO_2^- , and NO_3^- , and metal Fe in surface sediments, have been described by Zhang et al. (unpublished) (see Supplementary Methods). Briefly, with the increase of temperature, an obvious deoxygenation was observed in August (mean 2.94 mg L^{-1}), accompanied by a decrease of pH. The phytoplankton bloomed from June to August and faded after September. NH_4^+ concentration in sediments peaked in August, while NO_3^- was lowest in the hypoxic season. Among the sampling sites, the highest DO, but lowest salinity, sediment TOC, TN, and Fe content were detected at the nearshore site 16 with the coarsest grain size.

2.3. Nitrogen Fixation Rates Determination

The potential nitrogen fixation activity (NF) in sediments was determined by sediment-slurry incubation [7,23]. The slurry consisted of in situ fresh sediments and overlying water in a 1:7 ratio and was purged with high-purity helium for 30 min [23]. The slurry was then aliquoted into 12.5 mL vials using a syringe in a helium-filled environment. $^{30}\text{N}_2$ tracer (>99%, Shanghai Engineering Research Center of Stable Isotope, Shanghai, China) (0.6 mL) [7] was injected into the vials. A set of 6 vials was incubated per sediment sample, of which 3 vials were immediately spiked with 0.2 mL saturated ZnCl_2 as the initial samples and the remaining 3 vials were incubated in the dark under in situ temperature for 36 h followed by 0.2 mL of saturated ZnCl_2 as the stopping samples. After incubation, the initial and stopping samples were mixed again in a 100 mL centrifuge tube, respectively, degassed with helium for more than 25 min to exclude N_2 , and then repartitioned into initial and stopping vials followed by 400 μL of 4 M sodium hypobromite solution [24] to oxidize $^{15}\text{NH}_4^+$ produced by the nitrogen fixation process to $^{15}\text{N}_2$ ($^{29}\text{N}_2$ or $^{30}\text{N}_2$).

The standard curve was derived from the linear relationship between the known $^{15}\text{NH}_4^+$ (^{15}N , 99%, Shanghai Engineering Research Center of Stable Isotope, China) concentration (0, 5, 10, 15, and 20 μM) and the measured signal intensity of the total $^{15}\text{N}_2$ with $R^2 > 0.99$. Nitrogen fixation rate (F) was calculated by the following equation:

$$F = \frac{H_f - H_i}{t}$$

where H_i and H_f ($\mu\text{mol kg}^{-1}$) were the $^{15}\text{NH}_4^+$ content in the slurry before and after the reaction, respectively, and t (h) was the incubation time.

2.4. DNA Extraction and *nifH* Gene Quantification

Genomic DNA was extracted using a FastDNA[®] Spin Kit (MP Biomedicals, Irvine, CA, USA). The purity and concentration were detected using 1% agarose gel electrophoresis and the NanoDrop[®] spectrophotometer at 260 nm (Nanodrop 2000, Thermo Fisher Scientific, Waltham, MA, USA). The copy number of the *nifH* gene was determined through qPCR in triplicate on an ABI7500 Fast Real-Time PCR System (Applied Biosystems, Foster City, CA, USA) with an SYBR[®] GreenER[™] qPCR SuperMix (Thermo Fisher Scientific, Waltham, MA, USA), and about 342 bp fragments were amplified by the specific primer *polF* (5'-TGC GAY CCS AAR GCB GAC TC-3') and *polR* (5'-ATS GCC ATC ATY TCR CCG GA-3') [25]. The qPCR procedure is 95 °C 7 min, followed by 35 cycles of 95 °C 30 s, 56 °C 30 s, and 72 °C 1 min, and a default melting curve program. A qPCR standard curve was generated with serially diluted linearized plasmids containing the target *nifH* gene fragment. All qPCR experiments were completed with no-template controls. The correlation coefficients were above 0.99, and the amplification efficiencies were in the range of 90–110%. To confirm the specificity of qPCR primers and qPCR product size, qPCR products were validated by a melting curve and gel electrophoresis.

2.5. High Throughput Sequencing and Data Processing

The *nifH* gene community compositions were analyzed with Illumina sequencing with the same primer as qPCR using the MiSeq platform. The raw data were merged by Mothur v 1.30.1 [26] and filtered to obtain the clean data by the QIIME [27]. Usearch v 10 [28] was used to cluster tags to obtain OTU at a 97% similarity level, respectively, and the OTU was taxonomic annotated using RDP classifier v 2.2 [29] based on the FunGene database [30] with a minimum percentage identity cutoff of 80% for protein sequences and an e-value cutoff of 10^{-20} , and all unclassified reads were removed from the subsequent analyses. Alpha-diversity measurements, including Chao1 and Shannon diversity index, were calculated based on the rarefied OTU tables using the fewest sequences per sample. Beta diversity was determined with an edgeR package [31].

2.6. Statistical Analysis

Before analysis, all data were tested for normality by the Shapiro–Wilk normality test. Data that did not pass the normality test would be log-transformed. Statistical significance of NF rates, *nifH* abundance, alpha diversities, and relative abundances of microbial families and genera among different cruises and sampling sites was evaluated by one-way ANOVA followed by least significant difference (LSD). Spearman's or Pearson's correlation was used to assess relationships among environmental parameters, NF rates, and proportions of dominant microbial taxa. All the above analyses were performed using IBM SPSS (version 20.0). To evaluate the dissimilarity of diazotrophic community composition among different cruises and sampling sites, the non-metric multidimensional scaling (NMDS) analysis was used based on Bray-Curtis dissimilarities. Canonical correspondence analysis (CCA) was further employed to explore the explaining factors for diazotrophic community. CCA and NMDS were performed using PRIMER v.6 (PRIMER-E Ltd, Plymouth UK).

3. Results

3.1. Potential Nitrogen Fixation Rates

The NF rates across all sediment samples varied from 0.013 to 10.199 $\mu\text{mol kg}^{-1} \text{h}^{-1}$ and showed a significant spatial-temporal difference (Figure 2a,b). Among cruises, the highest rate of nitrogen fixation was observed in July ($3.2 \pm 3.41 \mu\text{mol kg}^{-1} \text{h}^{-1}$) and August ($2.27 \pm 2.49 \mu\text{mol kg}^{-1} \text{h}^{-1}$) during hypoxia, which was 3–4 folds higher than those in other months (ANOVA test, $p < 0.05$). When the section was concerned, site 18, S8, and S9 hosted much higher NF rates than other sites ($p < 0.05$).

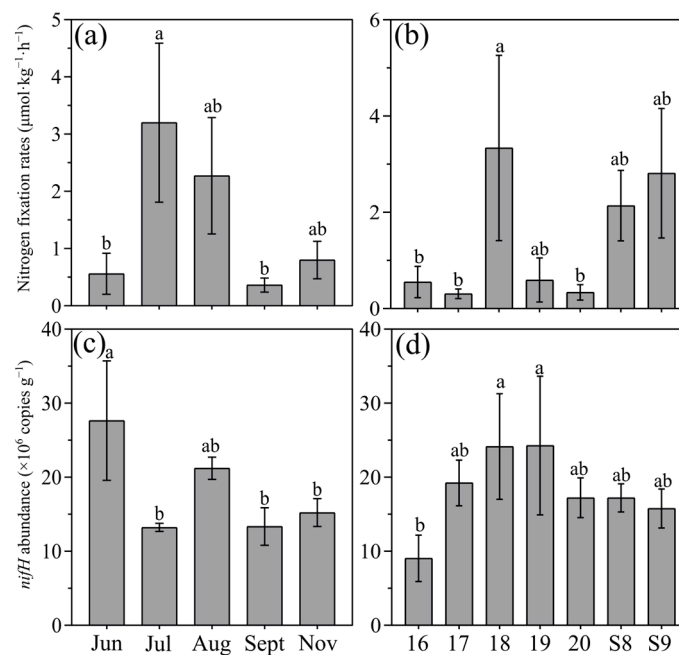


Figure 2. The variation of nitrogen fixation rates (a,b) and *nifH* gene abundance (c,d) among cruises and sampling sites in surface sediments from the Muping Marine Ranch. Different letters represent significant differences at $p < 0.05$ by ANOVA and LSD test in different cruises and sites.

3.2. Abundance of *nifH* Gene

The real-time qPCR analysis (Figure 2c,d) revealed that the *nifH* gene abundance in all sediment samples ranged from 2.90×10^6 to 61.03×10^6 copies g^{-1} wet sediment. The average *nifH* abundance peaked in June (on average 27.65×10^6 copies g^{-1} wet sediment), which was significantly higher than those in July, September, and November ($p < 0.05$), but was comparable to that in August (21.21×10^6 copies g^{-1} wet sediment). Among sampling sites, *nifH* gene abundance was significantly lower in the coastal site 16 ($(9.03 \pm 6.27) \times 10^6$ copies g^{-1} wet sediment) than in other sites (around 20×10^6 copies g^{-1} wet sediment) ($p < 0.05$).

3.3. Diversity, Composition, and Distribution of *nifH* Gene Community

A total of 1,719,592 high-quality reads were retained from all 35 sediment samples after quality control, and all reads were grouped into a total of 8950 OTUs at a 97% similarity threshold. There was no significant difference in Chao1 and Shannon indexes of *nifH* gene among different cruises (Figure 3a,c, $p < 0.05$). However, along the section (Figure 3b,d), the α -diversities of the *nifH* gene varied largely among sites. Site 16 possessed the lowest Chao 1 index (2454.87 ± 673.19) and the highest Shannon index (4.88 ± 0.26), while sites 17, 18, and 19 had higher both Chao1 and Shannon indexes ($p < 0.05$).

The compositions of *nifH* gene community at the family and genus levels are shown in Figure 4. Across all samples, over 60% of the *nifH* gene reads were derived from Geobacteraceae, followed by Desulfobulbaceae (13.61%), Bradyrhizobiaceae (9.29%), Desulfuromonadaceae (4.00%), and Desulfovibrionaceae (2.84%) at the family level. The other families were rare and accounted for less than 2.0%. At the genus level, more than 60%, and even 70%, of the *nifH* sequence came from *Geopsychrobacter*; other dominant genera (>5%) included *Desulfocapsa* and *Bradyrhizobium*. Overall, the main *nifH* taxa showed no significant seasonal pattern (Table S1, $p > 0.05$), except for *Desulfuromonas*, which had a higher proportion in September (5.55%) and lower in June (2.3%) ($p < 0.05$). Conversely, the most taxa presented significant site discrepancy (Table S1). For example, *Geopsychrobacter* and *Desulfocapsa* were enriched in site 20 (82.2%) and scarce in site 16 (18.0%). *Desulfocapsa* occurred frequently in site 17 (34.9%) and rarely in site S9 (2.4%) ($p < 0.05$).

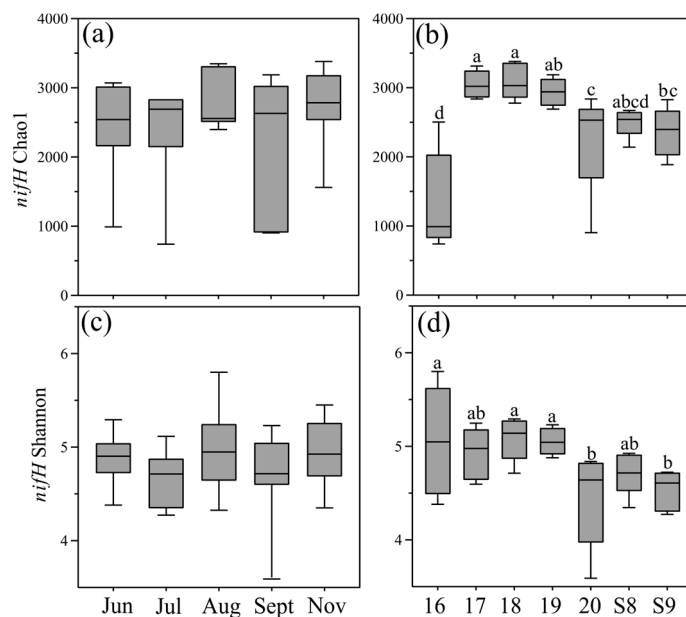


Figure 3. The variation of nitrogen fixation rates (a,b) and *nifH* gene abundance (c,d) among cruises and sampling sites in surface sediments from the Muping Marine Ranch. Different letters represent significant differences at $p < 0.05$ by ANOVA and LSD test in different cruises and sites.

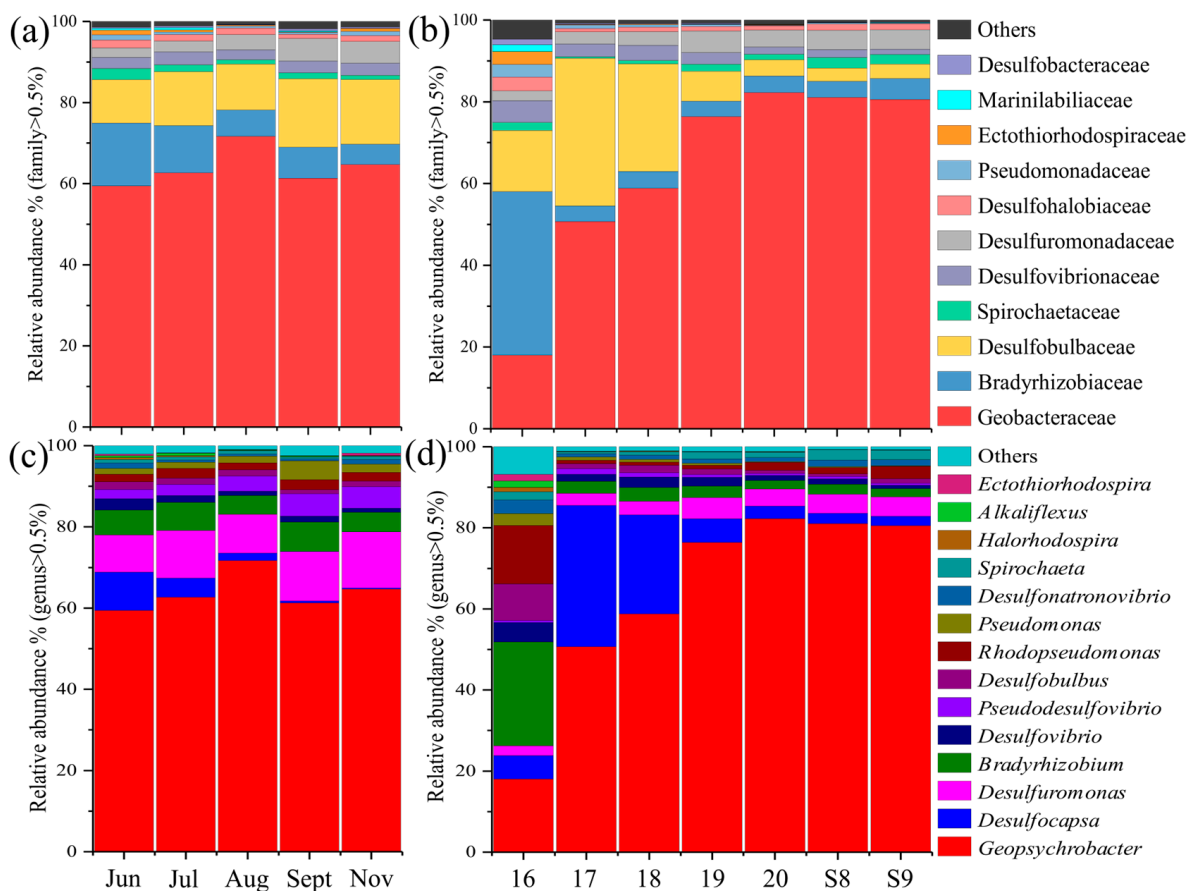


Figure 4. Columnar stacking diagram reflecting the relative abundance of the main taxa (average relative abundance > 0.5% across all samples) in *nifH* gene communities at the family (a,b) and genus levels (c,d).

The NMDS result further verified the site dissimilarity of *nifH* gene community structure (Figure 5). A clear separation in *nifH* gene community structure was revealed between 16 and other sites; in addition, samples from sites 17 and 18 were separated from those from sites 20, S8, and S9 (Figure 5). ANOSIM analysis supported that samples could be significantly separated among different sites ($R = 0.505$, $p = 0.001$) rather than different cruises ($R = -0.042$, $p = 0.846$).

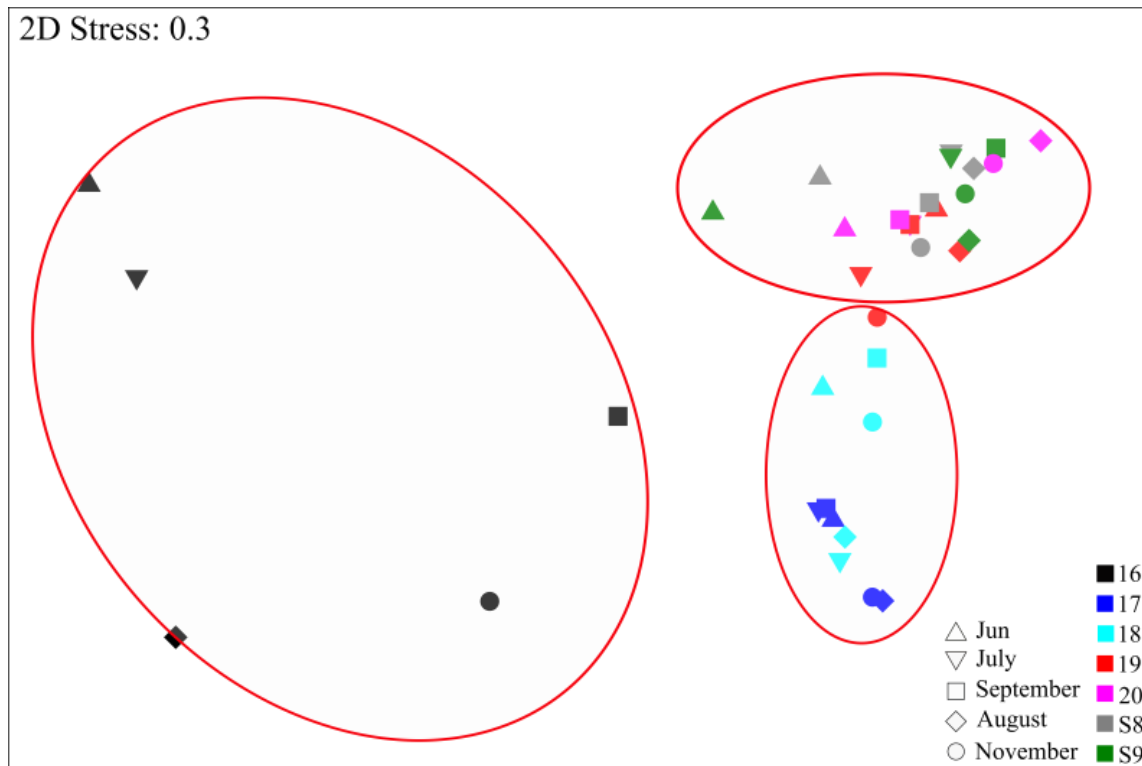


Figure 5. NMDS ordination of *nifH* microbial community with Bray–Curtis similarities for cruises and sites (stress value = 0.03).

3.4. Abundance of *nifH* Gene

Spearman's or Pearson's correlations showed that there was no significant relationship between sediment potential NF rates and any environmental factor determined across all samples ($n = 35$, $p > 0.05$). When the individual site or cruise was considered, we found that potential NF rates significantly positively correlated with the Chl-*a* concentration of overlying water in site 17 ($n = 5$, $R^2 = 0.971$, $p = 0.002$), and negatively correlated with sediment NH_4^+ level in site 18 ($R^2 = 0.775$, $p = 0.049$), and pH and DO of overlying water in site S9 ($R^2 > 0.45$, $p < 0.05$) (Figure 6).

Across all samples, the Chao1 index of the *nifH* gene had a negative correlation with sediment grain size ($n = 35$, $p < 0.001$, Figure 7a) and Fe content ($p = 0.049$), and a positive correlation with sediment TN ($p = 0.024$). The abundance of the *nifH* gene increased significantly with water depth ($p = 0.006$) and TOC and TN ($p < 0.05$), while it decreased with sediment grain size ($p = 0.001$) (Figure 7a). The relative abundance of *Geopsychrobacter* seemed to prefer finer sediments, higher sediment Fe, TN, TOC, NO_3^- , and deeper water ($p < 0.05$). *Desulfobulbus*, *Desulfovibrio*, *Desulfuromonas*, *Alkaliflexus*, *Desulfonatronovibrio*, *Halorhodospira*, and *Pseudomonas* exhibited the opposite correlations with these factors (Figure 7a, $p < 0.05$).

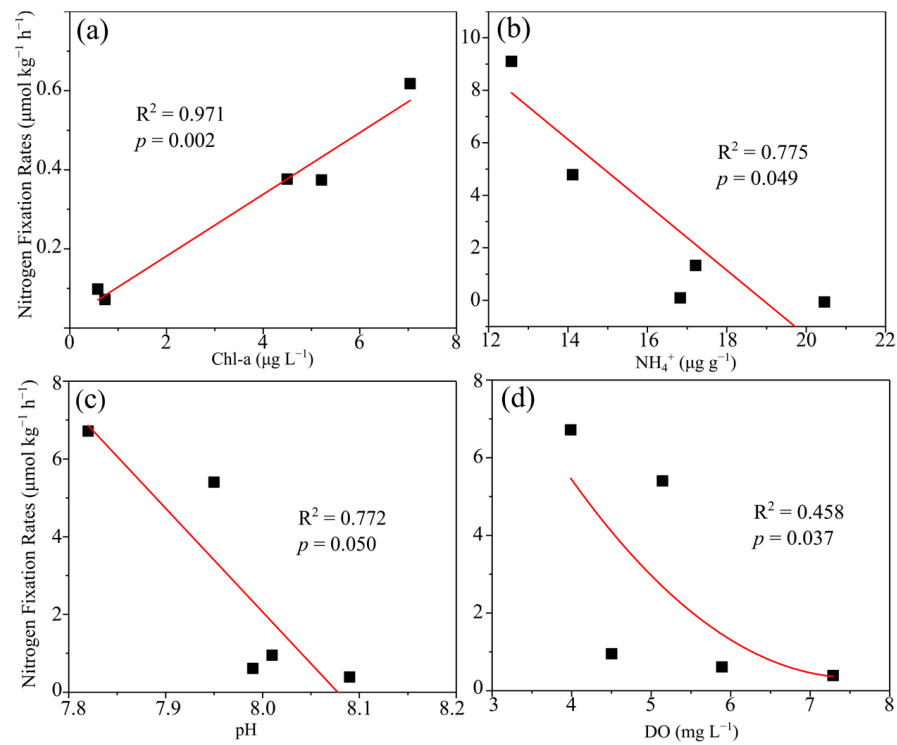


Figure 6. Scatter plots of significant correlations between nitrogen fixation rate and environmental parameter. (a) The correlation between NF and Chl-*a* content of overlying water at site 17. (b) The correlation between NF and sediment NH_4^+ at site 18. (c,d) The correlations of NF with overlying water pH and DO at site S9.

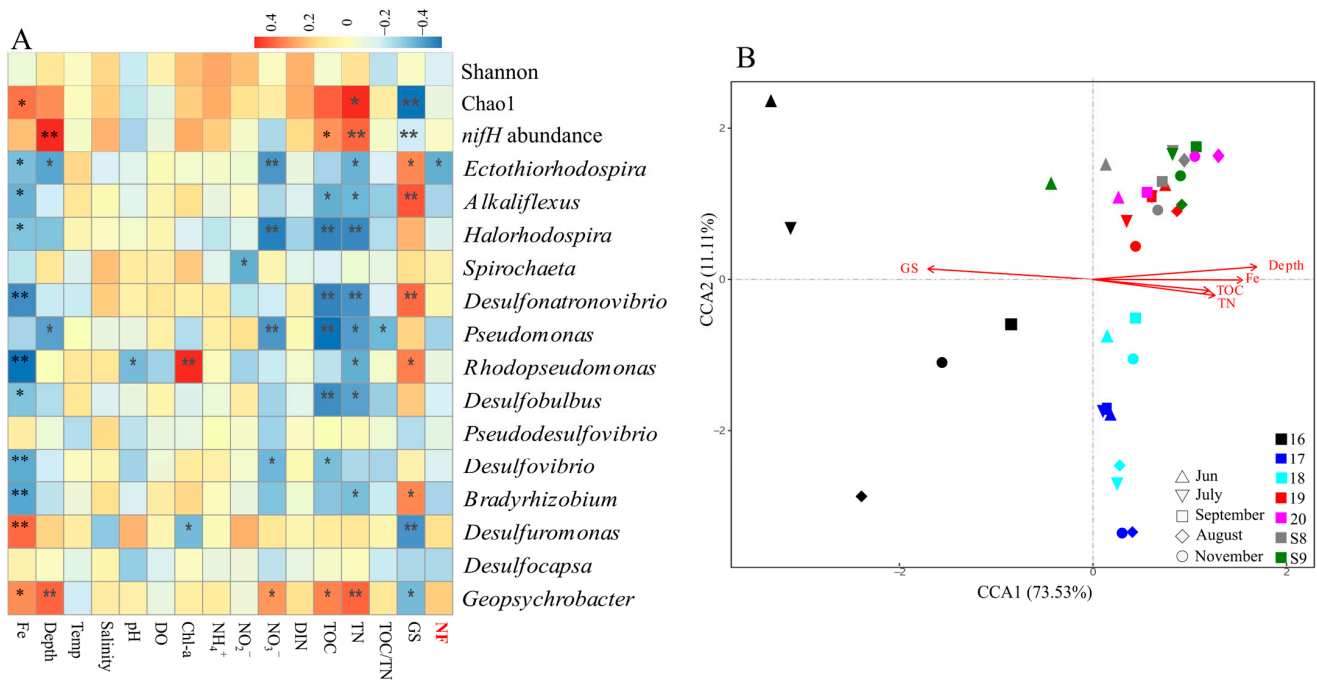


Figure 7. (A) Heatmap demonstrated correlations (Spearman’s or Pearson’s) of the *nifH* gene alpha-diversity index, abundance, and dominant groups with environmental factors and potential nitrogen fixation rates (NF). Significant correlation coefficient at * $p \leq 0.05$, ** $p \leq 0.01$. (B) Canonical correspondence analysis (CCA) shows the significant explaining factor for *nifH* gene community structure ($p < 0.05$).

As for the linking between NF rates and microbial traits, there was no statistical correlation between NF rates and *nifH* gene abundance or diversities ($n = 35$, $p > 0.05$, Figure 7a). On the other hand, the relative abundance of *Ectothiorhodospira* negatively related to nitrogen fixing activities ($p = 0.023$, Figure 7a). The canonical correlation analysis (CCA) revealed that the community structure of the *nifH* gene were primarily explained by Fe concentration, water depth, sediment TOC, TN, and grain size ($p = 0.001$) (Figures 7b and S2).

4. Discussion

4.1. Benthic Nitrogen Fixation Was Stimulated by Seasonal Hypoxia in Coastal Sediments

In this study, potential benthic NF rates ranged from 0.013 to 10.199 $\mu\text{mol kg}^{-1} \text{h}^{-1}$, i.e., 0.03–20.81 $\text{mmol N}_2 \text{m}^{-2} \text{d}^{-1}$ based on the average marine sediments density of 1.7 g cm^{-3} [32], with the average rate of 1.44 $\mu\text{mol kg}^{-1} \text{h}^{-1}$. The rates are comparable to the values reported from other estuarine and coastal sediments, such as the Yangtze Estuary (0.55–11.14 $\text{mmol N m}^{-2} \text{d}^{-1}$) [7], the coast of East China Sea (0.09–7.87 $\text{mmol N m}^{-2} \text{d}^{-1}$) [33], the Waquiot Bay (0–18.48 $\text{mmol N m}^{-2} \text{d}^{-1}$) [34], and the Gulf of Mexico hypoxic zone (0–3.53 $\text{mmol N m}^{-2} \text{d}^{-1}$) [10]. However, the rates are nearly three orders of magnitude higher than those (generally $<0.01 \mu\text{mol kg}^{-1} \text{h}^{-1}$) observed in open-sea benthic habitats ($>100 \text{ m}$ water depth) [35]. Greater organic carbon content in coastal habitats compared with open sea should be the primary reason for the higher N_2 fixation [35], since organic serve as suitable forms of carbon and electron donors for the diazotrophs [36].

A notable foundation in this study was that benthic N_2 fixation rates increased largely during hypoxia occurring in bottom water (July and August) (Figure 2a). In particular, a significant negative correlation between the nitrogen fixation rate and DO was observed in site S9 (Figure 6d), suggesting that seasonal hypoxia could enhance nitrogen fixation within the benthos of coastal ecosystems. Our results were supported by a recent study of Spinette et al. (2019) [37] in surface Narragansett Bay sediments, where benthic nitrogenase activity during summer hypoxia rose to 3–8 times of those under ambient conditions. In addition, the laboratory experiment with sediment core incubations also confirmed the boost of low oxygen to sediment N_2 fixation [37]. Similarly, in the eastern tropical South Pacific, nitrogen fixation activities were only detected in a small fraction of samples collected in subtoxic waters [38]. Luo et al. (2014) summarized N_2 fixation of 500 field measurements in Pacific and Atlantic oceans and found that subsurface minimum dissolved oxygen was a determining predictor explaining the spatial variance in the observed N_2 fixation data [39]. As oxygen is depleted in bottom water, oxygen penetration into sediments is reduced, thus promoting the activities of anaerobic sulfate reducers with nitrogen fixing potentials [40]. In addition, the nitrogenase is sensitive to oxygen, which was substantially inhibited by only 7 μM dissolved oxygen in pure culture [41]. Another possible explanation is that nitrogen fixation may also be triggered to supplement biologically active nitrogen removed by denitrification and anammox in the hypoxic zones [42]. Additionally, phosphorus from surface sediments is gradually released to pore water and overlying water under hypoxia conditions [43], indirectly promoting nitrogen fixation activity in hypoxic water bodies [44].

The availability of organic matter is another controlling factor for benthic NF activities in our study. Benthic NF rates at site 17 strongly positively correlated with Chl-*a* concentration in bottom water (Figure 6a), meaning that the influxes of autochthonous organic matter (algal residues) from the water column enhanced benthic nitrogen fixation. The stimulation of benthic NF with the addition of algal substrates has previously been noted by Spinette et al. (2019) [37], who demonstrated that benthic heterotrophic N fixation in coastal systems was generally carbon limited. In addition, Fulweiler et al. (2013) found that changes in the timing of algae blooms altered both the quantity and quality of organic matter loading to the benthos, and ultimately changed benthic NF rates [45]. In addition to being a carbon source and electron donor, the labile organic matter would increase the diversity and richness of diazotrophs [46].

A confounding issue remains in that the deposition of organic matter to sediments results in N remineralization processes, namely NH_4^+ is released; this would presumably

satisfy bacterial requirements for nitrogen and repress nitrogen fixation. In this study, the ammonium concentration showed significant negative correlation with the NF rate at site 18 (Figure 6b). This phenomenon is also observed within other oceanic sediments such as in Cochin Estuary [35,47] and the Swedish west coast [48]. Conversely, other studies have reported active N₂ fixation in sediments containing considerable amounts of NH₄⁺ [37,46,49], where it is conceivable that diazotrophs may exhibit fine-scale (mm) zonal distribution in micro-niches with low NH₄⁺ concentrations [15,37].

Aside from environmental factors, *nifH* gene abundance has usually been coupled with NF rates in previous studies [50,51]. On the contrary, no correlation between NF rates and *nifH* gene abundance was observed in this study (Figure 7a). A similar situation occurred in a study for nitrogen fixation in surface sediments of the East China Sea [33]. On one hand, some *nifH* genes detected could be silent (not expressed), and thus the levels of *nifH* gene transcript may be more representative [45,52]. Arashida et al. (2019) demonstrated that nitrogen fixation in some bacteria with the *nifH* gene does not take place when they are cultured under aerobic conditions [53]. On the other hand, the nitrogenase activity was also regulated by environmental factors rather than directly reflecting the NF rates [54]. For example, considerably high *nifH* gene abundance was observed in June in our research (Figure 2c), which had experienced an algae bloom in previous weeks. However, the NF potential rates peaked in July and August when oxygen was depleted (Figure 2a).

4.2. Iron-Reducing Bacteria Contributed Primarily to Benthic Nitrogen Fixation in the Coastal System

Based on high throughput sequencing of the *nifH* gene, Geobacteraceae are the most dominant nitrogen-fixer across all surface sediment samples (>60%, Figure 4). The Geobacteraceae have largely been categorized as facultative anaerobes that are important agents of oxidation of organics and certain metals coupled to the dissimilatory reduction of Fe (III) due to their advanced capacity for syntrophic metabolism and extracellular electron transfer [55]. They widely distribute in environments where active Fe (III) reduction takes place, such as rice paddies [56,57], wetlands [58], and landfill leachate-polluted aquifer [59]. Nitrogen fixation by Geobacteraceae has been detected in coastal sediments [60,61]. However, Geobacteraceae was seldom reported to comprise >50% of the *nifH* sequences obtained from coastal sediments over sulfate reducer, except in our study and Narragansett Bay sediments frequently stressed by seasonal hypoxia [62]. We speculated that the sedimentary environments with periodic changes in redox states should be key niches for Geobacteraceae, where reduced Fe (II) can be re-oxidized to Fe (III), supporting continuous electron acceptors for Geobacteraceae. Furthermore, their flexibility in the use of electron acceptors, namely utilizing alternative electron acceptors simultaneously, may help Geobacteraceae to deal with varying redox conditions and rapidly scavenge electron acceptors [63]. On the other hand, sediment pH was reduced by the release of large amounts of CO₂ accompanied by the occurrence of hypoxia, so Fe (III) was released more easily from the sediments [64]. These explanations were supported by our positive correlation between Geobacteraceae and Fe content in sediments (Figure 7).

Another abundant benthic diazotrophs was sulfate-reducing bacteria, including Desulfovibrionaceae, Desulfobacteraceae, Desulfobulbaceae, and Desulfobalobiaceae across all samples (Figure 4a,b). Sulfate-reducing bacteria have been reported as significant nitrogen-fixing microorganisms in various marine sediments [16,47], especially in organic-rich coastal sediments [46]. Degradation of organic matter by aerobic microbes consumes oxygen in sediments, nitrification was inhibited, and so sulfate becomes an important electron acceptor [65] for sulfate-reducing bacteria, which can further decompose organics under anaerobic conditions. This can explain the negative correlation between proportions of sulfate-reducing bacteria and sediment TN and TOC, and pore water NO₃⁻ concentration (Figure 7a).

Interestingly, sulfate-reducing bacteria showed completely opposite environmental responses to iron-reducing bacteria (Figure 7a). The result could be explained by a niche

complementarity effect between sulfate-reducing bacteria and Fe-reducing bacteria [66]. They can make full use of environmental resources to promote ecological environmental functions such as nitrogen fixation. There is a cooperative relationship on nitrogen fixation between the two groups: Fe (II), the product of iron reduction, can sink sulfides produced through sulfate reduction and promote nitrogen fixation by sulfate-reducing bacteria [67]. Therefore, we hypothesized that the joint action of iron- and sulfate-reducing bacteria contributed significantly to the biologically active nitrogen inputs to the eutrophic sediments in the seasonally hypoxic coastal zone.

Different from other offshore sampling sites, the most dominant diazotrophs at the coastal site 16 was *Bradyrhizobium* and *Rhodopseudomonas* (Figure 4d). *Bradyrhizobium* are widespread in terrestrial soils or freshwater sediments [68,69]. In some estuarine sediments, *Bradyrhizobium* were occasionally detected [46,70]. Two possible reasons could contribute the success of *Bradyrhizobium* at site 16: (i) *Bradyrhizobium*, an obligate aerobe, can utilize a broad range of oxygen levels but fix N₂ under very low oxygen tensions, which could explain the lower NF potential at site 16; (ii) river inputs could introduce *Bradyrhizobium* to the coastal site 16, which gradually get used to the coastal environments. Members of *Rhodopseudomonas* were well-known in treatment of aquaculture wastewaters [71], which could be carried into the coastal zone with the discharge of aquaculture wastewaters. In addition, many species of *Bradyrhizobium* have the ability to degrade the methoxychlor of organic pollutants such as aroma compounds and antibiotics [72]. Thus, besides potential N₂ fixation function, *Bradyrhizobium* and *Rhodopseudomonas* may contribute to pollutant degradation in nearshore regions.

4.3. Ecological Implication

In the present study, the mean benthic nitrogen fixation rate during the hypoxic period (July and August) was nearly five times that during the normoxic period. In other words, approximately 45.01 t N will be added into the Muping Marine Ranch (12.16 km²) over the two months due to the seasonal hypoxia. On the global ocean scale, hypoxic zones are expanding, and the duration of hypoxia is increasing. In accordance with our study, some previous studies have also showed that hypoxia events increased nitrogen fixation in eutrophic coastal zones [7,16,19]. These studies highlighted the importance of nitrogen fixation in coastal regions previously thought to be unfavorable for nitrogen fixation especially during hypoxia, and suggested that nitrogen fixation may play an important role in coastal hypoxic areas such as Pearl River estuary [73], Yangtze River Estuary [74], and Chesapeake Bay [75], which may be able to provide some complement data for global-scale nitrogen flux estimates about the imbalance between denitrification and nitrogen fixation.

However, the high nitrogen fixation during hypoxia counteracts the nitrogen removal by denitrification and anammox, which could further promote eutrophication in the water column and to some extent prolong the duration of algae blooms and worsen the hypoxic condition, forming a self-driven vicious cycle and making a significant impact on the economic efficiency of the marine ranching area (Figure 8). Therefore, a countermeasure is urgently needed to address this environmental problem, such as reducing anthropogenic organic inputs or accelerating consumption through economic algae farming to reduce the nutrient pressure of nitrogen and phosphorus in the marine ranch area.

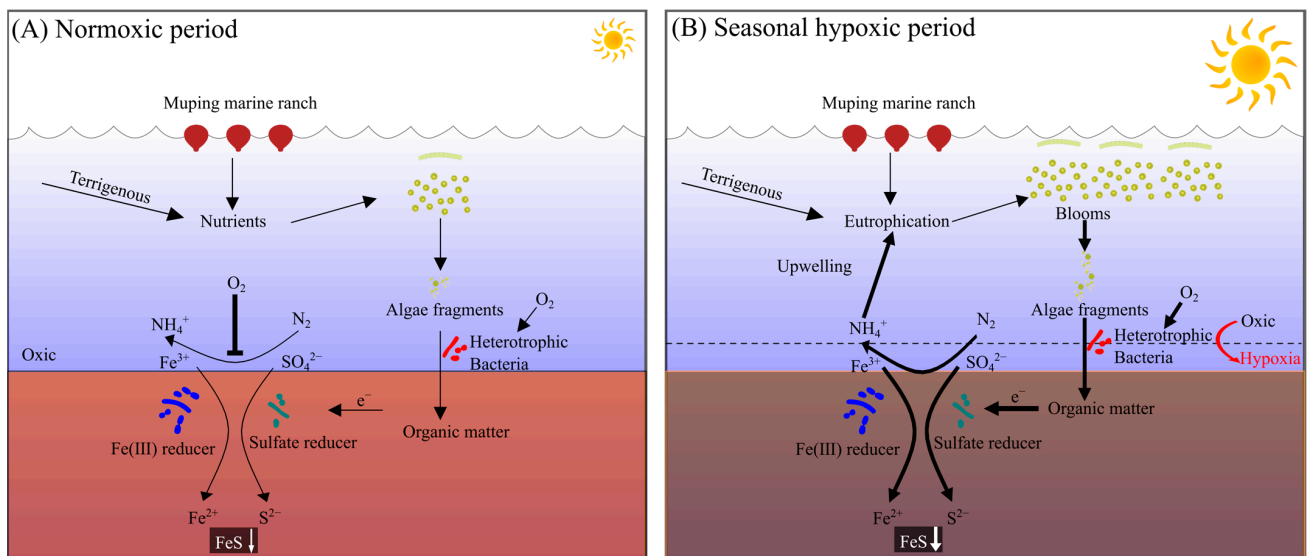


Figure 8. The patterns of benthic nitrogen fixation under (A) normoxic and (B) seasonal hypoxic conditions in Muping Marine Ranch. The thick arrows indicate higher fluxes and the symbol (\perp) represents inhibition.

5. Conclusions

In this study, we found that seasonal hypoxia substantially enhanced nitrogen fixation in benthos of a coastal marine ranch. Different from other coastal sediments, iron-reducing bacteria, Geobacteraceae, were the dominant diazotrophs in the marine ranch over sulfate-reducing bacteria. However, in the nearshore site, *Bradyrhizobium* and *Rhodospseudomonas* dominated the diazotrophic community. Besides oxygen, bottom water Chl-*a* concentration and pH, as well as sediment NH_4^+ contributed to the variation of benthic nitrogen fixation. However, sediment total organic carbon and nitrogen and Fe content significantly regulated diazotrophic abundance and communities. When hypoxia was occurring, iron-reducing bacteria could collaborate with sulfate-reducing bacteria to achieve the maximum nitrogen fixation efficiency. This study revealed the microbial mechanism of the N_2 fixation process responding to seasonal hypoxia, emphasized significant potential nitrogen fixation in the eutrophic marine ranch especially during hypoxia, and proposed some tips to alleviate the eutrophication of marine ranch and balance nitrogen cycling of the mariculture ecosystems.

Supplementary Materials: The following supporting information can be downloaded at: <https://www.mdpi.com/article/10.3390/pr11010138/s1>, Additional experimental methods of environmental parameters analysis; and additional tables. Table S1: Dissimilarity tests of *nifH* gene community among different cruises and different sites using One-way ANOVA. Table S2: Significance of environmental factors in explaining *nifH* gene community structure obtained from the CCA results. Refs. [76–78] are cited in Supplementary Materials.

Author Contributions: Conceptualization, J.Z. and X.Z.; Data curation, C.Y. and Q.Z.; Funding acquisition, J.Z. and X.Z.; Investigation, C.Y. and Q.Z.; Methodology, C.Y., Q.Z. and X.L.; Project administration, J.Z. and X.Z.; Resources, X.L.; Software, C.Y.; Supervision, X.L.; Validation, Q.Z.; Writing—original draft, C.Y. and Q.Z.; Writing—review & editing, J.Z. and X.Z. Finally, all authors reviewed and edited the manuscript prior to submission. All authors have read and agreed to the published version of the manuscript.

Funding: This work was funded by the National Science Foundation of China (No. 41976115, 41676154, 42276161), the Science and Technology Development Program of Yantai, China (2022XCZX103), and the Strategic Priority Research Program of the Chinese Academy of Sciences (XDA23050303).

Data Availability Statement: Not applicable.

Acknowledgments: The authors acknowledge Yongliang Liu and Chen Zhang for their help with field sampling and hydrographic data acquisition.

Conflicts of Interest: The authors declare no conflict of interest.

References

1. Gruber, N.; Galloway, J.N. An earth-system perspective of the global nitrogen cycle. *Nature* **2008**, *451*, 293–296. [[CrossRef](#)] [[PubMed](#)]
2. Wang, W.L.; Moore, J.K.; Martiny, A.C.; Primeau, F.W. Convergent estimates of marine nitrogen fixation. *Nature* **2019**, *566*, 205–211. [[CrossRef](#)] [[PubMed](#)]
3. Ward, B.A.; Dutkiewicz, S.; Moore, C.M.; Follows, M.J. Iron, phosphorus, and nitrogen supply ratios define the biogeography of nitrogen fixation. *Limnol. Oceanogr.* **2013**, *58*, 2059–2075. [[CrossRef](#)]
4. Zheng, M.; Chen, H.; Li, D.; Luo, Y.; Mo, J. Substrate stoichiometry determines nitrogen fixation throughout succession in southern Chinese forests. *Ecol. Lett.* **2020**, *23*, 336–347. [[CrossRef](#)] [[PubMed](#)]
5. Bentzon-Tilia, M.; Traving, S.J.; Mantikci, M.; Knudsen-Leerbeck, H.; Hansen, J.L.S.; Markager, S.; Riemann, L. Significant N₂ fixation by heterotrophs, photoheterotrophs and heterocystous cyanobacteria in two temperate estuaries. *ISME J.* **2015**, *9*, 273–285. [[CrossRef](#)] [[PubMed](#)]
6. Geisler, E.; Bogler, A.; Bar-Zeev, E.; Rahav, E. Heterotrophic nitrogen fixation at the hyper-eutrophic qishon river and estuary system. *Front. Microbiol.* **2020**, *11*, 1370. [[CrossRef](#)]
7. Hou, L.; Wang, R.; Yin, G.; Liu, M.; Zheng, Y. Nitrogen fixation in the intertidal sediments of the Yangtze estuary: Occurrence and environmental implications. *J. Geophys. Res. Biogeosci.* **2018**, *123*, 936–944. [[CrossRef](#)]
8. Rabalais, N.N.; Díaz, R.J.; Levin, L.A.; Turner, R.E.; Gilbert, D.; Zhang, J. Dynamics and distribution of natural and human-caused hypoxia. *Biogeosciences* **2010**, *7*, 585–619. [[CrossRef](#)]
9. Diaz Robert, J.; Rosenberg, R. Spreading dead zones and consequences for marine ecosystems. *Science* **2008**, *321*, 926–929. [[CrossRef](#)]
10. McCarthy, M.J.; Newell, S.E.; Carini, S.A.; Gardner, W.S. Denitrification dominates sediment nitrogen removal and is enhanced by bottom-water hypoxia in the northern gulf of Mexico. *Estuaries Coast* **2015**, *38*, 2279–2294. [[CrossRef](#)]
11. Ward, B.B.; Devol, A.H.; Rich, J.J.; Chang, B.X.; Bulow, S.E.; Naik, H.; Pratihary, A.; Jayakumar, A. Denitrification as the dominant nitrogen loss process in the Arabian Sea. *Nature* **2009**, *461*, 78–81. [[CrossRef](#)] [[PubMed](#)]
12. Kuypers, M.M.M.; Lavik, G.; Woebken, D.; Schmid, M.; Fuchs, B.M.; Amann, R.; Jørgensen, B.B.; Jetten, M.S.M. Massive nitrogen loss from the Benguela upwelling system through anaerobic ammonium oxidation. *Proc. Natl. Acad. Sci. USA* **2005**, *102*, 6478–6483. [[CrossRef](#)] [[PubMed](#)]
13. Thamdrup, B.; Dalsgaard, T.; Jensen, M.M.; Ulloa, O.; Farías, L.; Escibano, R. Anaerobic ammonium oxidation in the oxygen-deficient waters off northern Chile. *Limnol. Oceanogr.* **2006**, *51*, 2145–2156. [[CrossRef](#)]
14. Fernandez, C.; Farias, L.; Ulloa, O. Nitrogen fixation in denitrified marine waters. *PLoS ONE* **2011**, *6*, e20539. [[CrossRef](#)] [[PubMed](#)]
15. Gier, J.; Sommer, S.; Löscher, C.R.; Dale, A.W.; Schmitz, R.A.; Treude, T. Nitrogen fixation in sediments along a depth transect through the Peruvian oxygen minimum zone. *Biogeosciences* **2016**, *13*, 4065–4080. [[CrossRef](#)]
16. Bertics, V.J.; Löscher, C.R.; Salonen, I.; Dale, A.W.; Gier, J.; Schmitz, R.A.; Treude, T. Occurrence of benthic microbial nitrogen fixation coupled to sulfate reduction in the seasonally hypoxic Eckernförde Bay, Baltic Sea. *Biogeosciences* **2013**, *10*, 1243–1258. [[CrossRef](#)]
17. Messer, L.F.; Brown, M.V.; Van Ruth, P.D.; Doubell, M.; Seymour, J.R. Temperate southern Australian coastal waters are characterised by surprisingly high rates of nitrogen fixation and diversity of diazotrophs. *PeerJ* **2021**, *9*, e10809. [[CrossRef](#)]
18. Emil, V.; Daniel, J.C.; Bo, G.G.; Harri, K.; Heikki, P.; Oleg, P.S.; Timo, T.; Markku, V.; Maren, V.; Norbert, W.; et al. Internal ecosystem feedbacks enhance nitrogen-fixing cyanobacteria blooms and complicate management in the baltic sea. *AMBIO* **2007**, *36*, 186–194.
19. Hamersley, M.R.; Turk, K.A.; Leinweber, A.; Gruber, N.; Zehr, J.P.; Gunderson, T.; Capone, D.G. Nitrogen fixation within the water column associated with two hypoxic basins in the Southern California Bight. *Aquat. Microb. Ecol.* **2011**, *63*, 193–205. [[CrossRef](#)]
20. Yang, B.; Gao, X.; Zhao, J.; Lu, Y.; Gao, T. Biogeochemistry of dissolved inorganic nutrients in an oligotrophic coastal mariculture region of the northern Shandong Peninsula, north Yellow Sea. *Mar. Pollut. Bull.* **2020**, *150*, 110693. [[CrossRef](#)]
21. Sun, X.; Sun, X.; Zhu, L.; Li, X.; Sun, S. Seasonal and spatial variation in abundance of the copepod *Calanus sinicus*: Effects of decreasing dissolved oxygen and small jellyfish bloom in northern Yellow Sea, China, nearshore waters. *Mar. Pollut. Bull.* **2020**, *161*, 111653. [[CrossRef](#)]
22. Wang, L.; Liang, Z.; Guo, Z.; Cong, W.; Song, M.; Wang, Y.; Jiang, Z. Response mechanism of microbial community to seasonal hypoxia in marine ranching. *Sci. Total Environ.* **2022**, *811*, 152387. [[CrossRef](#)] [[PubMed](#)]
23. Li, X.; Hou, L.; Liu, M.; Zheng, Y.; Yin, G.; Lin, X.; Cheng, L.; Li, Y.; Hu, X. Evidence of nitrogen loss from anaerobic ammonium oxidation coupled with ferric iron reduction in an intertidal wetland. *Environ. Sci. Technol.* **2015**, *49*, 11560–11568. [[CrossRef](#)] [[PubMed](#)]
24. Naqvi, S.W.A.; Lam, P.; Narvenkar, G.; Sarkar, A.; Naik, H.; Pratihary, A.; Shenoy, D.M.; Gauns, M.; Kurian, S.; Damare, S.; et al. Methane stimulates massive nitrogen loss from freshwater reservoirs in India. *Nat. Commun.* **2018**, *9*, 1265. [[CrossRef](#)] [[PubMed](#)]

25. Poly, F.; Monrozier, L.J.; Bally, R. Improvement in the RFLP procedure for studying the diversity of nifH genes in communities of nitrogen fixers in soil. *Res. Microbiol.* **2001**, *152*, 95–103. [[CrossRef](#)] [[PubMed](#)]
26. Schloss, P.D.; Gevers, D.; Westcott, S.L. Reducing the effects of PCR amplification and sequencing artifacts on 16S rRNA-based studies. *PLoS ONE* **2011**, *6*, e27310. [[CrossRef](#)] [[PubMed](#)]
27. Caporaso, J.; Kuczynski, J.; Stombaugh, J.; Bittinger, K.; Bushman, F.; Costello, E.; Fierer, N.; Pena, A.; Goodrich, J.; Gordon, J.; et al. QIIME allows analysis of high-throughput community sequencing data. *Nat. Methods* **2010**, *7*, 335–336. [[CrossRef](#)]
28. Edgar, R.C. Search and clustering orders of magnitude faster than BLAST. *Bioinformatics* **2010**, *26*, 2460–2461. [[CrossRef](#)]
29. Wang, Q.; Garrity, G.M.; Tiedje, J.M.; Cole, J.R. Naive Bayesian classifier for rapid assignment of rRNA sequences into the new bacterial taxonomy. *Appl. Environ. Microbiol.* **2007**, *73*, 5261–5267. [[CrossRef](#)]
30. Fish, J.A.; Chai, B.; Wang, Q.; Sun, Y.; Brown, C.T.; Tiedje, J.M.; Cole, J.R. FunGene: The functional gene pipeline and repository. *Front. Microbiol.* **2013**, *4*, 291. [[CrossRef](#)]
31. Robinson, M.D.; McCarthy, D.J.; Smyth, G.K. Edger: A Bioconductor package for differential expression analysis of digital gene expression data. *Bioinformatics* **2010**, *26*, 139–140. [[CrossRef](#)] [[PubMed](#)]
32. Tenzer, R.; Gladkikh, V. Assessment of density variations of marine sediments with ocean and sediment depths. *Sci. World J.* **2014**, *2014*, 823296. [[CrossRef](#)] [[PubMed](#)]
33. Wang, R.; Li, X.; Hou, L.; Liu, M.; Zheng, Y.; Yin, G.; Yang, Y. Nitrogen fixation in surface sediments of the East China Sea: Occurrence and environmental implications. *Mar. Pollut. Bull.* **2018**, *137*, 542–548. [[CrossRef](#)] [[PubMed](#)]
34. Rao, A.M.; Charette, M.A. Benthic nitrogen fixation in an eutrophic estuary affected by groundwater discharge. *J. Coast Res.* **2012**, *28*, 477–485. [[CrossRef](#)]
35. Dekas, A.E.; Fike, D.A.; Chadwick, G.L.; Green-Saxena, A.; Fortney, J.; Connon, S.A.; Dawson, K.S.; Orphan, V.J. Widespread nitrogen fixation in sediments from diverse deep-sea sites of elevated carbon loading. *Environ. Microbiol.* **2018**, *20*, 4281–4296. [[CrossRef](#)]
36. Whaley-Martin, K.J.; Mailloux, B.J.; van Geen, A.; Bostick, B.C.; Silvern, R.F.; Kim, C.; Ahmed, K.M.; Choudhury, I.; Slater, G.F. Stimulation of microbially mediated arsenic release in bangladesh aquifers by young carbon indicated by radiocarbon analysis of sedimentary bacterial lipids. *Environ. Sci. Technol.* **2016**, *50*, 7353–7363. [[CrossRef](#)]
37. Spinette, R.F.; Brown, S.M.; Ehrlich, A.L.; Puggioni, G.; Deacutis, C.; Jenkins, B.D. Diazotroph activity in surface Narragansett Bay sediments in summer is stimulated by hypoxia and organic matter delivery. *Mar. Ecol. Prog. Ser.* **2019**, *614*, 35–50. [[CrossRef](#)]
38. Selden, C.R.; Mulholland, M.R.; Widner, B.; Bernhardt, P.; Jayakumar, A. Toward resolving disparate accounts of the extent and magnitude of nitrogen fixation in the Eastern Tropical South Pacific oxygen deficient zone. *Limnol. Oceanogr.* **2021**, *66*, 1950–1960. [[CrossRef](#)]
39. Luo, Y.W.; Lima, I.D.; Karl, D.M.; Deutsch, C.A.; Doney, S.C. Data-based assessment of environmental controls on global marine nitrogen fixation. *Biogeosciences* **2014**, *11*, 691–708. [[CrossRef](#)]
40. Muyzer, G.; Stams, A.J.M. The ecology and biotechnology of sulphate-reducing bacteria. *Nat. Rev. Microbiol.* **2008**, *6*, 441–454. [[CrossRef](#)]
41. Urdaci, M.C.; Stal, L.J.; Marchand, M. Occurrence of nitrogen fixation among *Vibrio* spp. *Arch. Microbiol.* **1988**, *150*, 224–229. [[CrossRef](#)]
42. Lam, P.; Kuypers, M.M.M. Microbial nitrogen cycling processes in oxygen minimum zones. *Annu. Rev. Mar. Sci.* **2011**, *3*, 317–345. [[CrossRef](#)] [[PubMed](#)]
43. Sulu-Gambari, F.; Hagens, M.; Behrends, T.; Seitaj, D.; Meysman, F.J.R.; Middelburg, J.; Slomp, C.P. Phosphorus cycling and burial in sediments of a seasonally hypoxic marine basin. *Estuaries Coast* **2018**, *41*, 921–939. [[CrossRef](#)]
44. Černá, B.; Rejmánková, E.; Snyder, J.M.; Šantrůčková, H. Heterotrophic nitrogen fixation in oligotrophic tropical marshes: Changes after phosphorus addition. *Hydrobiologia* **2009**, *627*, 55–65. [[CrossRef](#)]
45. Fulweiler, R.W.; Brown, S.M.; Nixon, S.W.; Jenkins, B.D. Evidence and a conceptual model for the co-occurrence of nitrogen fixation and denitrification in heterotrophic marine sediments. *Mar. Ecol. Prog. Ser.* **2013**, *482*, 57–68. [[CrossRef](#)]
46. Newell, S.E.; Pritchard, K.R.; Foster, S.Q.; Fulweiler, R.W. Molecular evidence for sediment nitrogen fixation in a temperate New England estuary. *PeerJ* **2016**, *4*, e1615. [[CrossRef](#)]
47. Jabir, T.; Vipindas, P.V.; Jesmi, Y.; Divya, P.S.; Adarsh, B.M.; Nafeesathul Miziriya, H.S.; Mohamed Hatha, A.A. Influence of environmental factors on benthic nitrogen fixation and role of sulfur reducing diazotrophs in a eutrophic tropical estuary. *Mar. Pollut. Bull.* **2021**, *165*, 112126. [[CrossRef](#)]
48. Andersson, B.; Sundbäck, K.; Hellman, M.; Hallin, S.; Alsterberg, C. Nitrogen fixation in shallow-water sediments: Spatial distribution and controlling factors. *Limnol. Oceanogr.* **2014**, *59*, 1932–1944. [[CrossRef](#)]
49. Knapp, A.N.; Casciotti, K.L.; Berelson, W.M.; Prokopenko, M.G.; Capone, D.G. Low rates of nitrogen fixation in eastern tropical South Pacific surface waters. *Proc. Natl. Acad. Sci. USA* **2016**, *113*, 4398–4403. [[CrossRef](#)]
50. Huang, J.; Xu, X.; Wang, M.; Nie, M.; Qiu, S.; Wang, Q.; Quan, Z.; Xiao, M.; Li, B. Responses of soil nitrogen fixation to *Spartina alterniflora* invasion and nitrogen addition in a Chinese salt marsh. *Sci. Rep.* **2016**, *6*, 20384. [[CrossRef](#)]

51. Tian, L.; Yan, Z.; Wang, C.; Xu, S.; Jiang, H. Habitat heterogeneity induces regional differences in sediment nitrogen fixation in eutrophic freshwater lake. *Sci. Total Environ.* **2021**, *772*, 145594. [[CrossRef](#)] [[PubMed](#)]
52. Caton, I.R.; Caton, T.M.; Schneegurt, M.A. Nitrogen-fixation activity and the abundance and taxonomy of nifH genes in agricultural, pristine, and urban prairie stream sediments chronically exposed to different levels of nitrogen loading. *Arch. Microbiol.* **2018**, *200*, 623–633. [[CrossRef](#)] [[PubMed](#)]
53. Arashida, H.; Kugenuma, T.; Watanabe, M.; Maeda, I. Nitrogen fixation in *Rhodospseudomonas palustris* co-cultured with *Bacillus subtilis* in the presence of air. *J. Biosci. Bioeng.* **2019**, *127*, 589–593. [[CrossRef](#)] [[PubMed](#)]
54. Wang, P.; Li, J.-L.; Luo, X.-Q.; Ahmad, M.; Duan, L.; Yin, L.-Z.; Fang, B.-Z.; Li, S.-H.; Yang, Y.; Jiang, L.; et al. Biogeographical distributions of nitrogen-cycling functional genes in a subtropical estuary. *Funct. Ecol.* **2022**, *36*, 187–201. [[CrossRef](#)]
55. Holmes, D.E.; Nevin, K.P.; Lovley, D.R. Comparison of 16S rRNA, nifD, recA, gyrB, rpoB and fusA genes within the family Geobacteraceae fam. *Nov. Int. J. Syst. Evol. Microbiol.* **2004**, *54*, 1591–1599. [[CrossRef](#)]
56. Li, L.; Jia, R.; Qu, Z.; Li, T.; Shen, W.; Qu, D. Coupling between nitrogen-fixing and iron (III)-reducing bacteria as revealed by the metabolically active bacterial community in flooded paddy soils amended with glucose. *Sci. Total Environ.* **2020**, *716*, 137056. [[CrossRef](#)]
57. Masuda, Y.; Itoh, H.; Shiratori, Y.; Isobe, K.; Otsuka, S.; Senoo, K. Predominant but previously-overlooked prokaryotic drivers of reductive nitrogen transformation in paddy soils, revealed by metatranscriptomics. *Microbes Environ.* **2017**, *32*, 180–183. [[CrossRef](#)]
58. Huang, X.; Yang, Q.; Feng, J.; Yang, Z.; Yu, C.; Zhang, J.; Ling, J.; Dong, J. Introduction of exotic species *Sonneratia apetala* alters diazotrophic community and stimulates nitrogen fixation in mangrove sediments. *Ecol. Indic.* **2022**, *142*, 109179. [[CrossRef](#)]
59. Lin, B.; Braster, M.; Röling, W.F.M.; van Breukelen, B.M. Iron-reducing microorganisms in a landfill leachate-polluted aquifer: Complementing culture-independent information with enrichments and isolations. *Geomicrobiol. J.* **2007**, *24*, 283–294. [[CrossRef](#)]
60. Jabir, T.; Vipindas, P.V.; Krishnan, K.P.; Mohamed Hatha, A.A. Abundance and diversity of diazotrophs in the surface sediments of Kongsfjorden, an Arctic fjord. *World J. Microb. Biotechnol.* **2021**, *37*, 41. [[CrossRef](#)]
61. Luo, Z.; Zhong, Q.; Han, X.; Hu, R.; Liu, X.; Xu, W.; Wu, Y.; Huang, W.; Zhou, Z.; Zhuang, W.; et al. Depth-dependent variability of biological nitrogen fixation and diazotrophic communities in mangrove sediments. *Microbiome* **2021**, *9*, 212. [[CrossRef](#)] [[PubMed](#)]
62. Brown, S.M.; Jenkins, B.D. Profiling gene expression to distinguish the likely active diazotrophs from a sea of genetic potential in marine sediments. *Environ. Microbiol.* **2014**, *16*, 3128–3142. [[CrossRef](#)] [[PubMed](#)]
63. Lin, B.; Westerhoff, H.V.; Roling, W.F. How Geobacteraceae may dominate subsurface biodegradation: Physiology of *Geobacter metallireducens* in slow-growth habitat-simulating retentostats. *Environ. Microbiol.* **2009**, *11*, 2425–2433. [[CrossRef](#)] [[PubMed](#)]
64. Lenz, C.; Jilbert, T.; Conley, D.J.; Slomp, C.P. Hypoxia-driven variations in iron and manganese shuttling in the Baltic Sea over the past 8 kyr. *Geochem. Geophys. Geosystems* **2015**, *16*, 3754–3766. [[CrossRef](#)]
65. Jessen, G.L.; Lichtschlag, A.; Ramette, A.; Pantoja, S.; Rossel, P.E.; Schubert, C.J.; Struck, U.; Boetius, A. Hypoxia causes preservation of labile organic matter and changes seafloor microbial community composition (Black Sea). *Sci. Adv.* **2017**, *3*, e1601897. [[CrossRef](#)]
66. Tilman, D.; Knops, J.; Wedin, D.; Reich, P.; Ritchie, M.; Siemann, E. The influence of functional diversity and composition on ecosystem processes. *Science* **1997**, *277*, 1300–1302. [[CrossRef](#)]
67. Holguin, G.; Vazquez, P.; Bashan, Y. The role of sediment microorganisms in the productivity, conservation, and rehabilitation of mangrove ecosystems: An overview. *Biol. Fertil. Soils* **2001**, *33*, 265–278. [[CrossRef](#)]
68. Noisangiam, R.; Nuntagij, A.; Pongsilp, N.; Boonkerd, N.; Denduangboripant, J.; Ronson, C.; Teamroong, N. Heavy metal tolerant *Metalliresistens boonkerdii* gen. nov., sp. nov., a new genus in the family Bradyrhizobiaceae isolated from soil in Thailand. *Syst. Appl. Microbiol.* **2010**, *33*, 374–382. [[CrossRef](#)]
69. Jin, C.-Z.; Wu, X.-W.; Zhuo, Y.; Yang, Y.; Li, T.; Jin, F.-J.; Lee, H.-G.; Jin, L. Genomic insights into a free-living, nitrogen-fixing but non nodulating novel species of *Bradyrhizobium sediminis* from freshwater sediment: Three isolates with the smallest genome within the genus *Bradyrhizobium*. *Syst. Appl. Microbiol.* **2022**, *45*, 126353. [[CrossRef](#)]
70. Thajudeen, J.; Yousuf, J.; Veetil, V.P.; Varghese, S.; Singh, A.; Abdulla, M.H. Nitrogen fixing bacterial diversity in a tropical estuarine sediments. *World J. Microbiol.* **2017**, *33*, 41. [[CrossRef](#)]
71. Kim, M.K.; Choi, K.-M.; Yin, C.-R.; Lee, K.-Y.; Im, W.-T.; Lim, J.H.; Lee, S.-T. Odorous swine wastewater treatment by purple non-sulfur bacteria, *Rhodospseudomonas palustris*, isolated from eutrophicated ponds. *Biotechnol. Lett.* **2004**, *26*, 819–822. [[CrossRef](#)] [[PubMed](#)]
72. Satsuma, K.; Masuda, M.; Sato, K. A role of *bradyrhizobium elkanii* and closely related strains in the degradation of methoxychlor in soil and surface water environments. *Biosci. Biotechnol. Biochem.* **2013**, *77*, 2222–2227. [[CrossRef](#)] [[PubMed](#)]
73. Li, X.; Lu, C.; Zhang, Y.; Zhao, H.; Wang, J.; Liu, H.; Yin, K. Low dissolved oxygen in the Pearl River estuary in summer: Long-term spatio-temporal patterns, trends, and regulating factors. *Mar. Pollut. Bull.* **2020**, *151*, 110814. [[CrossRef](#)]
74. Wang, B.; Wei, Q.; Chen, J.; Xie, L. Annual cycle of hypoxia off the Changjiang (Yangtze River) estuary. *Mar. Environ. Res.* **2012**, *77*, 1–5. [[CrossRef](#)] [[PubMed](#)]
75. Murphy, R.R.; Kemp, W.M.; Ball, W.P. Long-term trends in Chesapeake Bay seasonal hypoxia, stratification, and nutrient loading. *Estuaries Coast* **2011**, *34*, 1293–1309. [[CrossRef](#)]

76. Hou, L.; Zheng, Y.; Liu, M.; Gong, J.; Zhang, X.; Yin, G.; You, L. Anaerobic ammonium oxidation (anammox) bacterial diversity, abundance, and activity in marsh sediments of the Yangtze Estuary. *J. Geophys. Res. Biogeosci.* **2013**, *118*, 1237–1246. [[CrossRef](#)]
77. Carpenter, J.H. The Chesapeake Bay Institute Technique for The Winkler Dissolved Oxygen Method. *Limnol. Oceanogr.* **1965**, *10*, 141–143. [[CrossRef](#)]
78. Zhu, M.; Liu, J.; Yang, G.; Li, T.; Yang, R. Reactive iron and its buffering capacity towards dissolved sulfide in sediments of Jiaozhou Bay, China. *Mar. Environ. Res.* **2012**, *80*, 46–55. [[CrossRef](#)]

Disclaimer/Publisher’s Note: The statements, opinions and data contained in all publications are solely those of the individual author(s) and contributor(s) and not of MDPI and/or the editor(s). MDPI and/or the editor(s) disclaim responsibility for any injury to people or property resulting from any ideas, methods, instructions or products referred to in the content.